# Fast Penetration Resolving for Weft Knitted Fabric Based on Collision Detection

Sha Sha, Gaoming Jiang, Lisa Parrilo Chapman, Pibo Ma, Aijun Zhang, Honglian Cong, Qufu Wei, Zhijia Dong

Engineering Research Center for Knitting Technology, Jiangnan University, Wuxi, Jiangsu CHINA

Correspondence to:
Sha Sha email: sarah0323@sina.com

## ABSTRACT

In this paper, a hierarchical cylinders method is proposed to resolve penetration of yarns. The performance of the hierarchical cylinders method is accelerated by applying a spatial subdivision algorithm. The spatial subdivision algorithm refines the detected regions according to the properties of weft knitted fabric, which greatly reduce the calculation of collision detection. Based on the cuboid particle system, penalty contact forces act on the yarns with problematic penetration. Experimental results demonstrate that the proposed algorithm and method are efficient for weft knitted fabric simulation.

**Keywords**: Collision detection, yarn, hierarchical cylinders method, spatial subdivision, weft knitted fabric

## INTRODUCTION

Weft knitted fabric is widely used in clothing, industrial fabric and home textiles because of the aesthetic properties and comfortable stretch behavior，which is obviously different from the behavior of woven products. Unlike woven fabric, weft knitted fabric is seldom exhibited in animated effects. Modeling the visual appearance of weft knitted fabric is important for the sake of realism in computer graphics. Geometric modeling and deformation behavior are needed to represent the dimensional behavior of weft knitted fabric because it is essential to define the surface and physical properties in simulation. However, an essential task within the simulation process is the implementation of interactions between different yarns, where penetrations often occur. *Figure 1* shows that the penetration occurred when weft knitted fabric is exposed to external forces.

FIGURE 1. The penetration of weft knitted fabric.

Various methods to resolve the penetration/collision have been studied in the literature. Tens of thousands of mass elements were introduced into high quality woven fabric animations, which require many complicated calculations, such as numerous corresponding collisions and primitive pairs in close proximity [1, 2]. To simplify self-collision calculations, a curvature method was extracted by Provot [2], in which the hierarchy of subsurface regions were established. Many efficient collision detection methods track self-interactions in highly deformable surfaces [3-5]. Zhang et al. [6] used a particle pair system based on a mass-spring system to simulate yarn properties of woven fabrics under dynamic deformation. With the improvement of algorithms, the speed and stability of woven fabric animation has been significantly enhanced [7-9]. However, yarns are seldom used as the basic elements for collision detection in fabrics is seldom because of the amount of calculations required.

Kaldor et al. [10-12] proposed a simple plasticity model based on the resting state of a rod in angular space for approximating penalty-based contact forces in yarn-yarn collisions, and forces in nearby deformed configurations are approximated by a rotated linear force model. Durupınar and Güdükbay et al. [13, 14] used a particle-to-particle basis to deal with self-collisions, where penalty forces are calculated by the discrete element method (DEM). The methods discussed above lead to many advantages in quality and performance, but do not satisfy the real-time demand.

Cloth self-collision detection can be achieved using tests accelerated by bounding volume hierarchies (BVH), spatial subdivision, image-space techniques, Graphics Processing Unit (GPU)-based techniques, and distance field and hybrid algorithms [15-17]. Obviously, primary prior self-collision detection acceleration methods are constitutionally woven-based.

It is important to accurately detect yarns collisions because even a single missed collision can result in an invalid simulation and noticeable visual artifacts. The major objective of this work is to propose algorithms to resolve penetration between yarns. To reduce the cost of contact processing, a hybrid algorithm based on BVH and spatial subdivision is proposed. According to the features of weft knitted fabric, a collision spatial subdivision method is used to refine the region of collision detection. In order to solve problems which cannot generate factually physical deformation behavior of weft knitted fabric, a geometric model is built based on an improved cuboid particle system as the physical model. The geometric model is connected by Non-Uniform Rational B-Splines (NURBS) curves. These not only to resolve penetration but also improve the simulation performance of weft knitted fabric in terms of volumetric appearance and deformation behavior. The proposed algorithms are fast enough to act as an interactive system which simulates the deformation of weft knitted fabric without problematic penetration.

## PARTICLE DYNAMICS

The yarn-based particle system is an extension of Sha et al. [18]. The geometrical centerline of loop model is defined by NURBS curves $Q(u) = \frac{\sum_{i=0}^{n} \omega_i P_i N_{i,k}(u)}{\sum_{i=0}^{n} \omega_i N_{i,k}(u)}$, where $\omega_i$ is the weight factor, $P_i$ ($i$=0, 1,..., n) forms a control net, $N_i N_{i,k}(u)$ is the $k$ degree B-spline basic function, and $u_i$ is the node vector and $u_i = [u_0, u_1, \ldots, u_m]$. The geometric model is established on an improved mass-spring model which is referred to as the cuboid particle system in this work.

### Intra Particle System Properties

The mass-spring model [19] is widely employed to simulate deformations of woven fabric and knitwear [20]. To simulate volumetric performance and deformed behavior of fancy stitching in weft knitted fabric, the cuboid particle system is introduced in this work. Each face of the cuboid is modeled by stretching and shearing springs. Stitches in the weft knitted fabric are treated as bonding points whose coordinates are computed by interpolating those of neighboring 3-dimensional particles [18].

A weft knitted fabric undergoes deformation because particles are moved by forces which cause the bonding points move over time. The motion of bonding points results in deformation of weft knitted fabrics.

To calculate the intra-particle forces, a vector is representing interaction between particle $h(t, r, s)$ and the particle $h(t + \Delta t, r + \Delta r, s)$, can be defined as normalized vector $\varpi^m(t, r, s, \Delta t, \Delta r)$. Particles in arbitrary positions on the same surface are connected by stretching springs with vectors as $\varpi^m(t, r, s, \Delta t, \Delta r)$, such that:

$$\hat{\varpi}^m(t, r, s, \Delta t, \Delta r) = \frac{l^m(t + \Delta t, r + \Delta r, s) - l^m(t, r, s)}{\left| l^m(t + \Delta t, r + \Delta r, s) - l^m(t, r, s) \right|} \quad (1)$$

$$\varpi^m(t, r, s, \Delta t, \Delta r) = l^m(t + \Delta t, r + \Delta r, s) - l^m(t, r, s) \quad (2)$$

where $l^m(\mathrm{t}, r, s)$ is the position of $h(t, r, s)$. Similarly, $l^m(t + \Delta t, r + \Delta r, s + \Delta s)$ is the location of $h(t + \Delta t, r + \Delta r, s + \Delta s)$.

Intra-particle forces can be computed as:

$$\eta^{m}(t,r,s,\Delta t,\Delta r,\Delta s,\alpha_{\lambda},\beta_{\lambda}) = -a_{\lambda}\begin{pmatrix}\left(\left|\varpi^{m}(t,r,s,\Delta t,\Delta r)\right| - \left|\varpi^{0}(t,r,s,\Delta t,\Delta r)\right|\right) \\ \hat{\varpi}^{m}(t,r,s,\Delta t,\Delta r)\end{pmatrix} + b_{\lambda}\begin{pmatrix} v^{m}(t+\Delta t,r+\Delta r,s) \\ -v^{m}(t,r,s)\end{pmatrix}\hat{\varpi}^{m}(t,r,s,\Delta t,\Delta r) \quad (3)$$

In Eq. (3), the elasticity coefficient and damping coefficient are represented as $a_{\lambda}$ and $b_{\lambda}$ respectively, $v^{m}(t, r, s)$ and $v^{m}(t + \Delta t, r + \Delta r, s)$ are the current frame velocities of two connected particles.

**Penalty Contact Forces**

When the distances between any two detected points are less than the sum of the radius, contact forces should be added. The value of the force is:

$$C^{m}(t,r,s,\Delta t,\Delta r,\Delta s) = \frac{r^{m}(t,r,s)+r^{m}(t+\Delta t,r+\Delta r,s) - \left|l^{m}(t+\Delta t,r+\Delta r,s)-l^{m}(t,r,s)\right|}{\left|l^{m}(t+\Delta t,r+\Delta r,s)-l^{m}(t,r,s)\right| * [l^{m}(t+\Delta t,r+\Delta r,s)-l^{m}(t,r,s)]} * \hat{\varpi}^{m}(t,r,s,\Delta t,\Delta r) \quad (5)$$

Where $r^{m}(t,r,s)$ is the radius of $h(t, r, s)$. Similarly, $r^{m}(t+\Delta t,r+\Delta r,s+\Delta s)$ is the radius of $h(t + \Delta t, r + \Delta r, s + \Delta s)$.

**Time Integration**

The equation of motion of a particle resulting from internal contact forces is integrated using Velocity-Verlet integration, a velocity-free integration scheme. To avoid using the real-time location and velocity of a particle, Velocity-Verlet integration uses previous and current frame locations. Because it does not explicitly store the velocity of each particle, the Velocity-Verlet integration is much more stable than the Euler method and not as complex as implicit Euler method. The location and velocity of particles are:

$$l^{m+\Delta m}(t,r,s) = l^{m}(t,r,s) + v^{m+\Delta m}(t,r,s)\Delta m + \frac{(f_{total})^{m}(t,r,s)}{2M}\Delta m^{2} \quad (6)$$

$$v^{m+\Delta m}(t,r,s) = v^{m}(t,r,s)\Delta m + \frac{(f_{total})^{m} + (f_{total})^{m+\Delta m}}{2M}\Delta m \quad (7)$$

Where $m$ represents the current frame of particles under force, $\Delta m$ represents the time step duration, $M$ is the mass of each particle, $l^{m}(t, r, s)$ and $l^{m+\Delta m}(t, r, s)$ are the current and subsequent frames of particles. As the particles undergo force over time, the velocity and location of particles will be acquired.

## COLLISION DETECTION

In this section, a hybrid-based method is applied to detect collisions between yarns as well as potential collision regions in order to prevent yarn penetration and obtain real-time simulations.

**Potential Collision Regions**

Because some yarn segments cannot collide and comply with coherence requirements, the low collision regions need not be managed. In this work, according to the geometric properties of the loop model, spatial subdivision techniques are employed to identify the potential collision regions. Generally, the large regions are ignored. This dramatically improves the speed of animated simulation.

The potential collision regions should be defined by the geometric properties of the weft knitted loop model. The geometric loop model is shown in *Figure 2* and the potential collision regions are defined in *Figure* 3.

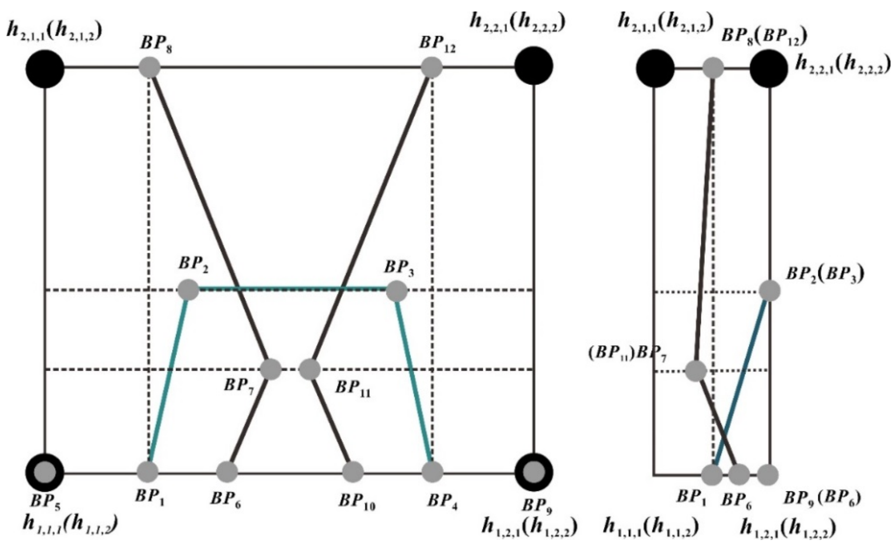


(a) Front view. (b) Left view.

FIGURE 2. The geometric loop model based on particle system.

The geometric model is composed of the top part of one yarn loop and the bottom part of the next row loop that is pulled through forming a loop. That means two rows of this model forms a complete loop. This model is much more independent since it connects only at single points between the unit loop, and it is usually relatively easy to create complicated stitches by composing such a model. The loop structure of the fabric is constructed by stitches which are composed of bonding points. The coordinates of the bonding points are computed by interpolating those of the neighboring particles. Based on the physical properties of the particles at the bonding points, the loop will deform as a function of the displacement of the particles.. The gray and black dots in *Figure 2* are bonding points and particles, and are denoted as $BP_s$ and $p_{i,j,k}$, respectively.

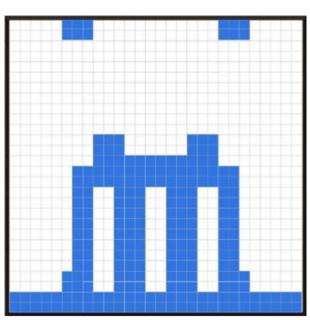

FIGURE 3. Potential collision regions of a loop unit.

In *Figure 3*, collisions are possible in the blue regions, but not in the white regions. Based on the geometric loop model and analysis of the relations between yarns, the potential collision regions of loop units can be subdivided into 28 columns and 28 rows, which is a one-to-one relationship with the geometric loop model. A subdivided region unit has the same height and width as the geometric model. Theoretically, the collisions will only occur in adjacent regions due to spring forces. Due to the frequent interlacing of the loop pillars, top arcs and sinker loops, collisions often appear in the bottom half of the geometric model. In contrast, collisions rarely occur in the top half of the geometric model. This is because distances between loop pillars are greater in the top half of the model. By using the spatial subdivision technique, the collision detection region is greatly reduced.

**Construction of Bounding Boxes**

To simulate the shape of the yarns and construct a bounding box, Raza and Kaldor et al. [12,21] used sphere superimposed along the axis of yarns. Their methods provide a realistic simulation, but a large amount of computation is required. In this work, it is assumed that the segments of yarns are cylinders that compose the yarns by rotation and translation, eliminating superimpositionm.

A number of points are inserted into two bonding points uniformly. These are distributed in the geometric centers of the yarns. Therefore, the lines connecting two adjacent interpolation points become the axes of cylinders. *Figure 4* shows the principle of the translation and rotation of the cylinder.

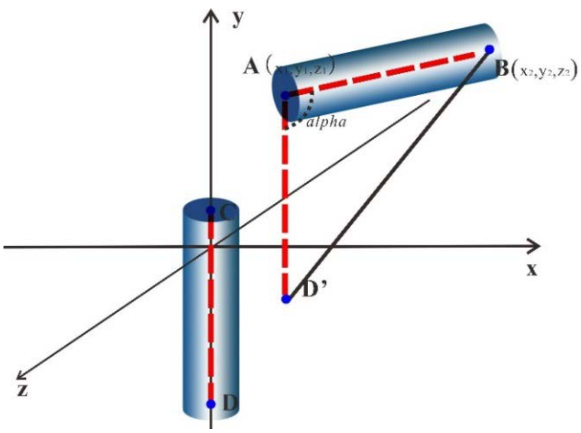


FIGURE 4. The principle of the translation and rotation of the cylinder.

From the above calculation, the coordinates of two interpolation points (A, B) can be obtained. The objective of this step is to rotate and translate the cylinder with CD as its axis to a position where the cylinder uses AB as its axis. The process consists of the following steps

i. Obtain the distance of $\overrightarrow{AB}$, designated as $\left|AB\right|$;
ii. Translate $\overrightarrow{CD}$ to $\overrightarrow{AD'}$, and calculate the value of translation ($x_1$, $y_1$, $z_1$) and the coordinate of D'. Therefore, the vector $\overrightarrow{AD'}$ is obtained;
iii. Calculate the normal vector of $\overrightarrow{AB}$ and $\overrightarrow{AD'}$ (it is denoted as ($n_x$, $n_y$, $n_z$)), the length of $\left|D'B\right|$ and *alpha*, which is the angle between $\overrightarrow{AD'}$ and $\overrightarrow{AB}$;
iv. The cylinder is moved to the target location using translation and rotation matrices.

**Collision Detection for Yarns**

There are three situations in which two cylinders could intersect: (a) a bottom face intersects with the other bottom face, (b) the flanks of the cylinders intersect orthogonally, (c) the intersection occurs at only one bottom face (oblique intersection).

In the first case, the bottom faces can be used directly for cylinder collision detection, as shown in *Figure* 5. $C_A$ and $C_B$ are the bottom faces of cylinders A and B, and the radii are denoted as $r_A$ and $r_B$, β is the angle of two planes $P_A$ and $P_B$ which $C_A$ and $C_B$ belong to, $d_A$ and $d_B$ are the distances of $C_A$ to $P_B$ and $C_B$ to $P_A$, respectively. The vectors $n_A$ and $n_B$ are the normal vectors of $P_A$ and $P_B$, $\sin\beta$ is the cross-product of normal vectors $n_A$ and $n_B$:

$$\sin\beta = \frac{\left|n_A \times n_B\right|}{\left|n_A\right|\left|n_B\right|} \tag{8}$$

Therefore, if $\sin\beta = 0$, it means that the two bottom faces are parallel and they cannot intersect. If the distance of the two centers $d$ satisfy the condition $d \le r_A + r_B$, the two bottom faces have intersected. Otherwise, only when conditions

$$r_A \times \sin\beta \ge d_A, r_B \times \sin\beta \ge d_B, d^2 \le r_A{}^2 + r_B{}^2$$

are satisfied, the two bottom faces have intersected.

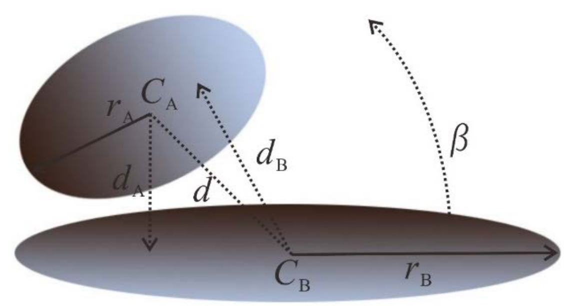


FIGURE 5. Lengths and angles involved in collision detections of spatial circles.

In the second and third cases, when the distance from the arbitrary generatrix of the cylinder 'A' to the axis of the cylinder 'B' is less than the radius of 'B', the cylinders intersect. Based on the above definitions, the axis $x_A$ is translated along the radius which points in the direction of the center of 'B'.

Therefore, the generatrix $g_A$ is obtained as shown in *Figure 6.* This is the closest generatrix to cylinder 'B'. Similarly, the generatrix $g_B$ which is closest to cylinder 'A' is obtained. If the two generatrices intersect, the two cylinders will intersect.

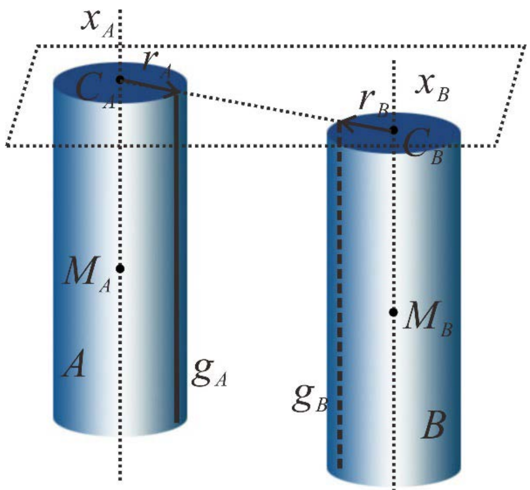


FIGURE 6. Method of obtaining the generatrix.

If the generatrices do not intersect, there are two possible scenarios, as shown in *Figure 7*. To distinguish between the two, vertical lines between $x_A$ and between $g_B$ and $x_B$ to $g_A$ are drawn. The vertical lines are denoted as $v_A$ and $v_B$. Then $v_A$ and $v_B$ are compared with $r_A$ and $r_B$ using the following algorithm.

It is assumed that two straight lines $l_1$ and $l_2$ in different planes pass through points ($x_1$, $y_1$, $z_1$) and ($x_2$, $y_2$, $z_2$), respectively. The direction vectors are ($d_1$, $e_1$, $f_1$) and ($d_2$, $e_2$, $f_2$), respectively. The outer product of the two direction vectors $p$ is:

$$p:\ (A, B, C) = \left[\begin{vmatrix} e_1 & f_1 \\ e_2 & f_2 \end{vmatrix}, -\begin{vmatrix} d_1 & f_1 \\ d_2 & f_2 \end{vmatrix}, \begin{vmatrix} d_1 & e_1 \\ d_2 & e_2 \end{vmatrix}\right] \quad (9)$$

The determinant of $D$, $N_1$, $N_2$ is:

$$D = \begin{vmatrix} A & B & C \\ d_1 & e_1 & f_1 \\ d_2 & e_2 & f_2 \end{vmatrix}, N_1 = \begin{vmatrix} A & B & C \\ x_2 - x_1 & y_2 - y_1 & z_2 - z_1 \\ d_2 & e_2 & f_2 \end{vmatrix}, \quad (10)$$
$$N_1 = \begin{vmatrix} A & B & C \\ d_1 & e_1 & f_1 \\ x_2 - x_1 & y_2 - y_1 & z_2 - z_1 \end{vmatrix}$$

Therefore, the endpoints of common vertical lines are:

$$T_1 : \left( x_1 + \frac{m_1 N_1}{D}, y_1 + \frac{n_1 N_1}{D}, z_1 + \frac{p_1 N_1}{D} \right);$$
$$T_2 : \left( x_2 + \frac{m_2 N_2}{D}, y_1 + \frac{n_2 N_2}{D}, z_1 + \frac{p_2 N_2}{D} \right); \quad (11)$$

The Euclidean distance from $T_1$ to $T_2$ is $d_{Euclidean} = |T_2 - T_1|$. Similarly, $d_{EuclideanA}$ and $d_{Euclidean\ B}$ can be calculated. If $d_{EuclideanA} \le r_B$ or $d_{EuclideanB} \le r_A$, the two cylinders intersect, as shown in *Figure 7(a).* Otherwise, the two cylinders are separated, as shown in *Figure 7(b).*

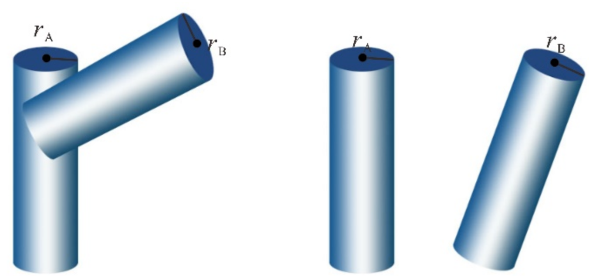


(a) The cylinders intersect. (b) The cylinders do not intersect.

FIGURE 7. Two possible scenarios resulting from non-intersecting generatrices.

## RESULTS AND DISCUSSION

To evaluate the performance of the algorithms for collision detection of weft knitted fabrics, the algorithms and methods are implemented and compared with existing methods. The simulation is performed using a system with an Intel XEON Processor E3-123v3 LGA1150, 3.30 GHz, 16 GB RAM, and GTX 690 running on Windows 7 OS. The software platform is Microsoft Visual Studio 2010 integrated development tools with an OpenGL 3-D graphics library. In these experiments, the algorithms are compared with the most widely used hierarchical bounding boxes methods: the hierarchical sphere method and axis-aligned bounding boxes method (AABB). The hierarchy of bounding boxes is constructed from bottom to top by spatial subdivision. The smallest bounding boxes of the set of elements are calculated. In this work, the hierarchical cylinders are chosen as the bounding volume boxes. *Table I* shows the computational times of collision detection for weft knitted fabric simulations. $V_1$ is the hierarchical cylinders used in this work, $V_2$ is the AABB hierarchical method, and $V_3$ is the hierarchical sphere method.

In a collision detection method using spatial subdivision, an efficient and flexible data structure is important. In this work, the queue template "deque" of the Standard Template Library (STL) is applied in order to construct the bidirectional queue, to which elements can be added or deleted arbitrarily. As mentioned above, the external forces acting on fabric and internal forces acting on tuck stitches are simulated. Therefore, yarn penetration is resolved efficiently, as shown in *Figure 8*.

The proposed algorithms and methods can resolve the penetration occurring in weft knitted fabric simulation. Combining the cuboid particle system and the hierarchical cylinders method, the deformation of forced weft knitted fabric can be simulated through animation.

TABLE I. Computational times of collision detection for weft knitted fabric simulations.

| Figure | $V_1$ (ms) | $V_2$ (ms) | $V_3$ (ms) |
|---|---|---|---|
| 8(a) | 40.4 | 33.4 | 45.2 |
| 8(b) | 34.5 | 26.3 | 39.3 |
| 8(c) | 57.1 | 48.7 | 61.7 |

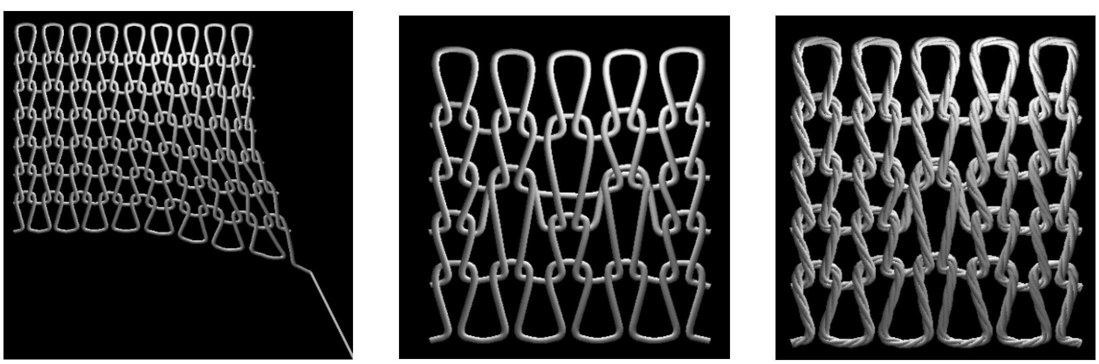

(a) External forces act on fabric. (b) Internal forces act on tuck stitches. (c) Internal forces act on tuck stitches with yarn twist.

FIGURE 8. Penetration resolved by applying collision detection.

## CONCLUSION

In this paper, algorithms and methods are proposed to resolve the penetrations among weft knitted fabrics. The detected areas are positioned by spatial subdivision according to the properties of the fabric. Hierarchical cylinders methods are applied as the bounding boxes to detect collision, and the penetrations are treated using penalty contact forces. Algorithms describing the yarn-based collision detection are implemented. The consumed time and screenshots taken from the simulations in this work have demonstrated that the proposed methods offer an effective real-time treatment useful in modifying the penetration of weft knitted fabric.

**ACKNOWLEDGMENT**
The authors acknowledge the financial support from the National Science Foundation of China (No.11302085 and No. 51403080), Fundamental Research Funds for the Central Universities (No. JUSRP51404A, No. JUSRP51625B and No. JUSRP115A02), the Natural Science Foundation of Jiangsu Province (No. BK20151129), the Innovation Program for Graduate Education in Jiangsu Province (No. KYLX15_116), Innovation fund project of CIUI (Cooperation among Industries, Universities & Research Institutes) Jiangsu Province (No. BY2015019-31), and the State Scholarship Fund from China Scholarship Council (201500090098), a project funded by the Priority Academic Program Development of Jiangsu Higher Education Institutions（PAPD).

**REFERENCES**

[1] Baraff, D.; Witkin, A. and Kass, M.; Untangling cloth; *ACM TRANSACTIONS ON GRAPHICS* 2003, 22, 862-870.

[2] Provot, X.; Collision and self-collision handling in cloth model dedicated to design garments; *Computer Animation and Simulation '97: Proceedings of the Eurographics Workshop* 1997, 177-189.

[3] Kimmerle, S.; Nesme, M. and Faure, F.; Hierarchy accelerated stochastic collision detection; *Proceedings of Vision, Modeling, Visualization* 2004, 307-314.

[4] Baciu, G.; Image-Based Collision Detection for Deformable Cloth Models; *Ieee Transactions on Visualization and Computer Graphics* 2004, 10, 649-663.

[5] Govindaraju, N. K.; Knott, D.; Jain, N.; Kabul, I. and Tamstorf, R.; Interactive collision detection between deformable models using chromatic decomposition; *ACM TRANSACTIONS ON GRAPHICS* 2005, 24, 991-999.

[6] Zhang, J.; Baciu, G.; Cameron, J. and Hu, J. L.; Particle pair system: An interlaced mass-spring system for real-time woven fabric simulation; *Textile Research Journal* 2012, 82, 655-666.

[7] Zhong, Y. and Xu, B.; Three-dimensional Garment Dressing Simulation; *Textile Research Journal* 2009, 79, 792-803.

[8] Zhong, Y.; Redressing Three-dimensional Garments Based on Pose Duplication; *Textile Research Journal* 2010, 80, 904-916.

[9] Zhong, Y.; Fast Penetration Resolving for Multi-layered Virtual Garment Dressing; *Textile Research Journal* 2009, 79, 815-821.

[10] Kaldor, J.; James, D. and Marschner, S.; Simulating Knitted Cloth at the Yarn Level; *Proceedings of SIGGRAPH 2008* 2008,8, 1-9.

[11] Kaldor, J. M. Simulating yarn-based cloth. Cornell University 2011.

[12] Kaldor, J. M.; James, D. L. and Marschner, S.; Efficient yarn-based cloth with adaptive contact linearization; *ACM TRANSACTIONS ON GRAPHICS* 2010, 29, 1.

[13] Durupınar, F. and Güdükbay, U.; Procedural visualization of knitwear and woven cloth; *Computers & Graphics* 2007, 31, 778-783.

[14] Gudukbay, U.; Bayraktar, S.; Koca, C. and Ozguc, B.; Particle-based simulation of the interaction between fluid and knitwear; *Signal Image and Video Processing* 2014, 8, 415-422.

[15] Teschner, M.; Kimmerle, S.; Heidelberger, B. and Zachmann, G.; Collision detection for deformable objects; *In Computer Graphics Forum* 2005, 24, 61-81.

[16] Ji, F.; Simulate the Dynamic Draping Behavior of Woven and Knitted Fabrics; *Journal of Industrial Textiles* 2006, 35, 201-215.

[17] Sul, I. H.; Fast cloth collision detection using collision matrix; *International Journal of Clothing Science and Technology* 2010, 22, 145-160.

[18] Sha, S.; Jiang, G.; Ma, P. and Li, X.; 3-D dynamic behaviors simulation of weft knitted fabric based on particle system; *Fibers and Polymers* 2015, 16, 1812-1817.

[19] Provot, X.; Deformation constraints in a mass-spring model to describe rigid cloth behavior; *Graphics Interface '95* 1995, 147-154.

[20] Meißner, M. and Eberhardt, B.; The art of knitted fabrics,realistic physically based modelling of knitted patterns, C355-C362. Siddiqui, M. and Sun, D.; Porosity Prediction of Plain Weft Knitted Fabrics; *Fibers* 2014, 3, 1-11.

**AUTHORS' ADDRESSES**
**Sha Sha**
**Gaoming Jiang**
**Lisa Parrilo Chapman**
**Pibo Ma**
**Aijun Zhang**
**Honglian Cong**
**Qufu Wei**
**Zhijia Dong**
Engineering Research Center for Knitting Technology
Ministry of Education
Jiangnan University
No. 1800, Lihu Road
Wuxi, Jiangsu 214122
CHINA